JOURNAL OF CHEMICAL INFORMATION AND MODELING

Article

pubs.acs.org/jcim

Ligand−Receptor Affinities Computed by an Adapted Linear Interaction Model for Continuum Electrostatics and by Protein Conformational Averaging

Ariane Nunes-Alves and Guilherme Menegon Arantes*

Department of Biochemistry, Instituto de Química, Universidade de São Paulo, Av. Prof. Lineu Prestes 748, 05508-900, São Paulo, SP, Brazil

Supporting Information

ABSTRACT: Accurate calculations of free energies involved in small-molecule binding to a receptor are challenging. Interactions between ligand, receptor, and solvent molecules have to be described precisely, and a large number of conformational microstates has to be sampled, particularly for ligand binding to a flexible protein. Linear interaction energy models are computationally efficient methods that have found considerable success in the prediction of binding free energies. Here, we parametrize a linear interaction model for implicit solvation with coefficients adapted by ligand and binding site relative polarities in order to predict ligand binding free energies. Results obtained for a diverse series of ligands suggest that the model has good predictive power and transferability. We also apply implicit ligand theory and propose approximations to average contributions of multiple ligand−receptor poses built from a protein conformational ensemble and find that exponential averages require proper energy discrimination between plausible binding poses and false-positives (*i.e.*, decoys). The linear interaction model and the averaging procedures presented can be applied independently of each other and of the method used to obtain the receptor structural representation.

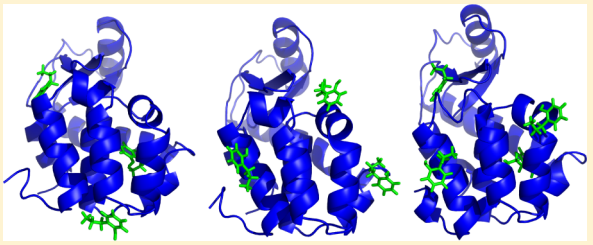

1. INTRODUCTION

Prediction of binding affinities between small-molecule ligands and protein receptors has both fundamental and applied importance.[1] In practice, this is a very challenging task[2] because the ligand functional or bound configurations have a small energy difference from the huge amount of alternative ligand unbound configurations.[3] The number and strength of contributions in the ligand bound and unbound states are similar. Consequently, intermolecular interactions have to be evaluated with accuracies much better than 1 kcal mol^{-1} to discriminate the small energy gap between the two states.[3,4] In addition, a huge number of configurations has to be generated and their energy calculated to sample the important conformational microstates of the molecular system.[3,5,6] The number of configurations to be sampled will increase if the protein or the ligand has a more flexible structure and if their binding pose is unknown or not unique.[2,7]

Despite the challenges, there has been enormous progress in the prediction of binding free energies, and several methods have been proposed to tackle the problem.[1,8,9] In one hand, the application of detailed all-atom force fields, molecular dynamics (MD) simulations (or related approaches), and rigorous free energy estimators[10−13] have found impressive agreement with experimental affinities;[14−17] but, given the high computational costs associated, these methods have been successfully applied mainly to less flexible proteins and ligands for which binding sites are known or easy to determine.[18] The high computational costs still prohibit these rigorous methods from being applied in screenings of large ligand sets. On the other hand, molecular docking[19−21] employs approximate descriptions of intermolecular interactions usually parametrized against empirical data and efficient conformational search methods to generate binding poses,[22,23] rank or enrich ligand sets,[24,25] and determine ligand affinities.[2,26] However, docking has many documented failures[27,23,28] which may be due to severe approximations in the calculation of interactions and lack of transferability for ligands or receptors not included in the method parametrization as well as to insufficient conformational sampling.

Another family of methods shows accuracy and computational ease in between the two approaches just mentioned. They are called linear interaction energy (LIE) models[29−32] because a linear response of the intermolecular interactions[33] is assumed in the estimation of binding free energies by the equation

$$\Delta G_{LIE} = \alpha\Delta\langle V_{vdW}^{l-e}\rangle + \beta\Delta\langle V_{elet}^{l-e}\rangle + \gamma \quad (1)$$

where a force field description of intermolecular van der Waals (*vdW*) and electrostatic (*elet*) interactions between ligand and its environment (V^{l-e}) is employed. The difference (Δ) of ensemble averaged ($\langle\cdots\rangle$) interactions between the ligand free state (when environment is the solvent only) and bound state (when environment is the solvated protein complex) is

Received: May 19, 2014
Published: July 30, 2014

multiplied by coefficients derived from the linear response assumption (β) or fit to empirical data (α and γ).[32,34]

LIE models have been applied successfully to predict affinities for a range of ligand−receptor complexes.[32,35−38] However, in many of these applications, the LIE models were specifically parametrized to the system studied. In order to increase the model transferability, Hansson et al. proposed the adaptation of coefficients to ligand properties (e.g., the number of possible hydrogen bonds).[39] Recently, Linder et al. suggested an adaptative LIE model where coefficients in eq 1 are adjusted by the relative polarities of the ligand and of the binding cavity achieving accuracy and model transferability.[40]

To increase computational efficiency and to avoid the sometimes slow convergence of explicit solvent contributions[41,42] in eq 1, continuum electrostatics descriptions of solvation[43−46] have been used in LIE models.[36,41,47−49] Here, we propose and describe the necessary parametrization of LIE models that combine an implicit solvent description with adaptative coefficients[40] to predict binding affinities. Local configurational sampling of ligand−receptor complexes usually done by molecular dynamics simulations is substituted by more economic molecular docking and geometry optimizations.[21,36,47]

The methods mentioned so far rely their predictions on one initial receptor structure, typically obtained from X-ray crystallography. During conformational search in molecular docking, the receptor structure is maintained rigid, maybe allowing for side-chain rotations or smoothened interactions.[50−52] In methods applying ensemble averages, protein configurations near the initial structure are visited in relatively short MD simulations; but, for flexible receptors, sufficient sampling of protein motions will be difficult to achieve in both approaches. A possible solution in those cases is to start the search or averaging from a conformational ensemble, i.e., from multiple representations of the receptor structure.[6,7,53,54]

Several approaches, mostly related to docking, are now used to predict binding poses and affinities from receptor conformational ensembles.[22,55−59] Usually a dominant pose and dominant state approximation is applied.[57−59] This means that the binding free energy or the related docking score for a given ligand−receptor pair is estimated from the most favorable pose (only one) found after evaluating several complexes obtained from the different receptor structures in the ensemble. This approximation should be appropriate for the level of accuracy expected in docking, but it dismisses important contributions such as multiple binding poses, receptor reorganization energy and thermal fluctuations, and the related entropic effects. Thus, it may be useful to average contributions obtained from an ensemble of ligand−receptor poses.[60,61]

Based on the implicit ligand theory recently developed,[61] two ensemble averages can be defined for the calculation of binding free energy between a ligand and a receptor represented by a conformational ensemble embedded in an implicit solvent. The first average concerns with the ligand configurational distribution that may be obtained for interaction with one given *rigid* receptor structure. It has been called the binding potential of mean-force, B, and may be estimated by an exponential mean

$$B = -k_B T \ln \frac{1}{P} \sum_{i=1}^{P} \exp\left(-\frac{\Psi_i}{k_B T} \right) \quad (2)$$

where k_B is the Boltzmann constant, T is the temperature, P is the number of ligand configurations sampled, and Ψ_i is the *implicit solvent-mediated* interaction energy for the ith ligand pose.[61]

The second ensemble average accounts for the receptor configurational distribution. Similarly, it may be estimated by an exponential mean, leading to an expression for the binding free energy

$$\Delta G_{ave} = -k_B T \ln \frac{1}{N} \sum_{n=1}^{N} \exp\left(-\frac{B_n}{k_B T} \right) + \Delta G_{\xi} \quad (3)$$

where B_n is the binding potential of mean-force (eq 2) for the nth receptor configuration out of a total of N configurations sampled.[61] ΔG_{ξ} represents a correction to standard concentration due to restriction of the volume sampled by the ligand.

Here, we propose approximations to these two exponential averages in order to account for multiple binding poses and for protein conformation flexibility. In the next section, we provide details of the training and test sets and the methodology used to calibrate adapted LIE models for continuum solvation. System setup, generation of receptor−ligand poses, and definition of the force fields employed are also described. Both Results and Discussion are divided in two parts. First, we report the construction and performance of the adapted LIE models and the procedures for averaging contributions from an ensemble of ligand−receptor poses. Then, we analyze the accuracy and shortcomings of the proposed LIE model as well as the applicability of the ligand−receptor conformational averaging.

2. COMPUTATIONAL METHODS

Calibration and tests of the proposed approximations were conducted using bacteriophage T4 lysozyme mutants L99A[62] and L99A/M102Q,[17,63] HIV-1 reverse transcriptase (HIVRT), and human FK506 binding protein 12 (FKBP) as model systems (Table 1). These proteins were chosen based on the availability of experimental structures and binding affinities. The ligand set varies in size from fragment-like small molecules which bind T4 lysozyme to lead-like molecules which bind FKBP. Only neutral ligands were considered (Table S3 and Figure S1 in the Supporting Information, SI).

Table 1. Proteins Included in the Training and Test Sets and Ranges of Binding Affinities of Associated Ligands (in kcal mol^{-1})

protein[a]	PDB code	ligands	$-\Delta G_{exp}$
L99A	3DMV	benzene derivatives	4.5−6.7
M102Q	1LI3	benzene derivatives	4.3−5.8
HIVRT	1RT1	HIV1−HIV6	4.9−11.8
FKBP	1FKG	FKB1−FKB5	7.8−11.2

[a]T4 lysozyme mutants L99A and M102Q, HIV-1 reverse transcriptase (HIVRT), and human FK506 binding protein 12 (FKBP).

2.1. Parametrization of the Model. Following Linder et al.,[40] system-derived descriptors are used here to scale coefficients in the linear interaction models. Ligand (π) and cavity or binding site (η) relative polarities were given by the ratio PSA/SA, where SA represents the ligand or cavity total surface area and PSA represents the area of its subset of polar atoms (Table S3 and Table S4). Ligand surface area was obtained from the "3V" server,[64] and ligand polar surface area

was calculated using the approach of Ertl et al.[65] Cavity area was obtained from the *SA* of residues in contact with (or less than 4 Å from) the ligand. Thus, each binding pose has a characteristic η. Protein carbonyl C, O, N, and H bound to O and N were assigned as polar atoms.[66]

Coefficients in the LIE equations were obtained by an optimization procedure that minimized deviations between calculated and experimental affinities for a training set of 10 T4 lysozyme ligands, 3 HIVRT ligands, and 10 T4 lysozyme false-positive poses, as indicated in Table S5. The test set used to check the performance of the parametrized equations was composed of a different set of 15 T4 lysozyme binders, 10 T4 lysozyme false-positive poses, 9 T4 lysozyme nonbinders, 3 HIVRT ligands, and 5 FKBP ligands, as indicated in Table 2. Optimization was carried out with a combination of genetic (GA)[67] and simplex[68] algorithms as previously described.[69] A population of 10 individuals with each coefficient represented by 12 bits was used in the GA. Coefficients in eq 6 could vary between [0,10] for k_S, [−20,20] for k_6, and [−10,10] for the others k_i (eqs 6 and S1−S3). Populations evolved for 10^6 generations. Simplex optimization was carried from the best GA individuals until the difference in deviations between successive generations was smaller than 10^{-6} kcal mol^{-1}.

2.2. Construction of Receptor−Ligand Structures. Protein structures retrieved from the Protein Databank (PDB) were used after removal of water and other crystallization molecules. Incomplete side chains were built with the WHATIF server.[70] Hydrogens were constructed using the GROMACS PDB parser[71] for proteins and Babel 2.2[72] for ligands. Ligand geometry was optimized using Gaussian[73] with the AM1[74] potential if holo crystal structures were unavailable.

To train and test the LIE models, holo structures were taken from the PDB when available. Otherwise, the most favorable binding pose obtained from docking the ligand to an apo structure was used (Table S3). These poses were compared to known crystal structures of congeneric ligands bound to the same protein to confirm the docked ligand was complexed in a plausible binding mode.

Unstable or artificial poses of known binders may be generated in docking due to inaccuracies in the scoring functions.[27,28,75] Such artificial poses, here called false-positives, were used as a decoy set to assist in the parametrization of the LIE equations. Assuming the ligand will occupy a site different from the known crystallographic site, false-positive poses were obtained by docking ligands to apo crystal structures using a grid excluding the known binding site. Selected poses were submitted to energy minimization, careful heating up ramps, and 10−20 ns explicit solvent molecular dynamics simulations as described below. False-positive poses were retained only if the ligand spent more than 20% of the trajectory dissociated from the protein. Ligand-protein dissociation was monitored by the ligand solvent accessible surface area (SASA).

Tentative configurational ensembles were generated for apo T4 lysozyme L99A and M102Q mutants, HIVRT bound to ligand HIV1 and FKBP bound to ligand FKB1 (Table 1). Ensembles generated from apo HIVRT and FKBP could not be used for docking due to large conformational changes which occluded the binding sites (see Discussion for further details). Receptor structures were submitted to energy minimization, and implicit solvent molecular dynamics simulations were run for 160−235 ns. For each protein, an ensemble was constructed by 50 configurations (excluding the ligand in the case of HIVRT and FKBP) collected along trajectories at regular time intervals (3−4 ns) after stabilization of C_α root mean-squared deviation (RMSD). For each configuration in an ensemble, 20 docking poses were generated resulting in a total of 1000 ligand-bound structures for each protein−ligand pair.

Dockings to crystal structures were performed with AutoDock 4.0[50] with its genetic algorithm search run with 150 individuals for 27,000 generations maximum. Dockings to

Table 2. Binding Free Energies (in kcal mol^{-1}) Experimentally Measured and Estimated by Eq 6 for the Ligand *Test Set*

ligand	ΔG_{exp}[a]	ΔG_{ALICE}
L99A		
n-butylbenzene[b]	−6.7	−6.3
propylbenzene	−6.5	−5.7
ethylbenzene[b]	−5.7	−5.1
toluene	−5.5	−3.7
benzene[b]	−5.2	−3.0
3-ethyltoluene	−5.1	−5.5
meta-xylene	−4.7	−4.5
2-ethyltoluene	−4.5	−4.8
propylbenzene	>−2.0	−1.4
ortho-xylene (A)	>−2.0	0.7
toluene	>−2.0	−1.7
4-ethyltoluene	>−2.0	−2.1
benzene	>−2.0	−0.8
3-methylpyrrole	>−2.0	−2.6
phenol	>−2.0	−3.1
1,3,5-trimethylbenzene	>−2.0	−4.4
cyclohexane	>−2.0	−2.6
2-fluoroaniline	>−2.0	−2.8
M102Q		
(phenylamino)acetonitrile[b]	−5.8	−4.8
toluene	−5.2	−4.1
3-methylpyrrole	−5.2	−2.9
thieno[3,2-b]thiophene[b]	−4.9	−3.5
2-ethylphenol[b]	−4.8	−5.0
catechol[b]	−4.4	−2.5
2-ethoxyphenol[b]	−4.3	−4.9
thieno[3,2-b]thiophene	>−2.0	−0.3
(phenylamino)acetonitrile	>−2.0	−0.4
catechol	>−2.0	−2.4
2-propylphenol (A)	>−2.0	−1.7
2-ethoxyphenol	>−2.0	−0.7
phenylhydrazine	>−2.0	−3.0
2-methoxyphenol[b]	>−2.0	−4.5
4-vinylpyridine	>−2.0	−4.2
N-(*o*-tolyl)cyanoformamide	>−2.0	−5.0
HIVRT		
HIV3	−8.1	−10.5
HIV4	−10.6	−9.5
HIV5	−6.4	−7.4
FKBP		
FKB1[b]	−11.0	−10.9
FKB2[b]	−11.2	−11.4
FKB3	−7.8	−7.2
FKB4	−8.5	−7.8
FKB5	−9.6	−9.9

[a]Repeated from Table S3. [b]Holo structure taken from the PDB. False-positive poses of binder molecules are underlined. These poses and nonbinders were assumed to have $\Delta G_{exp} > -2.0$ kcal mol^{-1}. The label (A) represents different false-positive poses of the same ligand.

dx.doi.org/10.1021/ci500301s | J. Chem. Inf. Model. 2014, 54, 2309−2319

the configurational ensemble were done with AutoDock Vina[21] setting the exhaustiveness level to 8. Conformational search options were chosen in order to thoroughly search for the possible docking poses in a given protein structure. Grids with 0.375 Å spacing and 60 to 80 points were centered in the known binding sites. Protein structures were kept frozen, but bond torsions were allowed in ligands. Typically, T4 lysozyme ligands had 0−4 torsions activated, HIVRT ligands had 3−12 torsions, and FKBP ligands had 6−13 torsions (Table S2). The correction of the restricted volume sampled by the ligand to the standard concentration (1 M)[60] in eq 3 was calculated from the average volume of the grid used for docking, 2.7×10^4 Å^3.

2.3. Protein Force Field and Simulation Details. Energy contributions for the linear interaction models (eqs 6 and S1−S3) were obtained after geometry optimizations of protein−ligand complexes in implicit solvent using the conjugate gradient approach (T4 lysozyme) or the BFGS algorithm (HIVRT and FKBP).[68] Free protein and ligand contributions were obtained without the ligand or protein, respectively, but using the same geometry of the complex. The GBr^6 method[43] was used to calculate the solvent polarization free energies, G_{GB} in eq 6.

GROMACS 4.5[71] was used for all protein geometry optimizations and MDs. Dynamics were carried out at 300 K with a 2 fs time-step, and covalent bonds were constrained with LINCS.[76] Proteins were represented by the OPLS-AA force field.[77]

In explicit solvent simulations, structures were solvated in a dodecahedral box with edges at least 8 Å far from the protein. The SPC/E potential[78] was employed for water, and chloride ions were added to neutralize the charge of the systems. Periodic boundary conditions were activated. The velocity rescale method[79] was used to control the temperature at 300 K, and pressure control at 1 bar was applied with the Parrinello−Rahman method.[80] PME[81] was used to treat long-range electrostatics, and a switched potential (cutoffs 0.8, 1.2 nm) was used to treat van der Waals interactions. Before production MD, systems were heated in cycles of short 20 ps simulations with gradual temperature increase (10 K, 50 K, 100 K, 200 K, and 300 K) and reduction of position restraints over heavy atoms (240 kcal nm^{-2}, 120 kcal nm^{-2}, 24 kcal nm^{-2}, 2 kcal nm^{-2}, and 0).

In implicit solvent simulations, the generalized Born (GB) approximation was used.[44] The OBC model was used to estimate Born radii,[45] and the nonpolar contribution was calculated as in Schaefer et al.[46] with a surface tension of 5.4 cal mol^{-1} Å^{-2} for all atoms. MDs were run with a leapfrog stochastic dynamics integrator, with a friction coefficient $\tau = 10$ ps^{-1}.

2.4. Ligand Force Field. Topologies for ligands were built manually based on the OPLS-AA force field. Bonding, Lennard-Jones, and implicit solvation parameters unavailable for certain atom types in OPLS-AA were approximated from similar chemical functions. Parameters for dihedral angles of the thymine ring in HIVRT ligands were taken from the AMBER99 force field[82,83] OPLS-AA partial charges were used for nonpolar ligands or for ligands with one polar group. For ligands with more than one polar group, partial charges were recalculated with AM1-CM2.[74,84] For small ligands, partial charges for the whole molecule were recalculated. For the bulky FKBP and HIVRT ligands, the molecule was divided in fragments, and those with more than one polar group had their partial charges recalculated. For HIVRT ligands containing sulfur, the partial charges were recalculated with HF/6-31G*.

For all ligands, the partial charges used here resulted in total and component dipole moments in good agreement with a quantum mechanical (QM) reference (HF/6-31G*, Table S1). For instance, OPLS-AA partial charges were used for 4-vinylpyridine resulting in a total dipole moment $\mu = 2.7$ D which is in good agreement with the QM reference $\mu = 2.6$ D. Another example is 2-fluoroaniline which has two polar groups. Its partial charges were recalculated as described above and resulted in $\mu = 2.0$ D which is in good agreement with the QM reference, $\mu = 1.9$ D.

All ligand topologies are available online[85] or from the authors upon request.

2.5. Approximations to Implicit Ligand Theory. Given that only configurations with favorable interaction energies will contribute significantly to the exponential average in eq 2, here we use ligand docking to quickly generate ligand−receptor poses with favorable interactions for a rigid receptor conformation and approximate $\Psi \approx \Delta G_{int}$. Thus, eq 2 leads to

$$B_E = -k_B T \ln \frac{1}{P} \sum_{i=1}^{P} \exp\left(- \frac{\Delta G_{\mathrm{int},i}}{k_B T} \right) \quad (4)$$

where ΔG_{int} is an intrinsic binding free energy used to estimate the stability of a given ligand binding pose (see Results, section 3.1). As docking does not generate an equilibrium distribution of ligand−receptor configurations, application of eq 4 is approximate. Substitution of interaction energies (Ψ in eq 2) for an intrinsic binding free energy parametrized against experimental data may partially correct inaccuracies in the docking energy function and introduce entropic contributions.

In the limit that one individual sample dominates the exponential average in eq 4, the dominant pose approximation may be used

$$B_D = \min_i (\Delta G_{\mathrm{int},i}) \quad (5)$$

where only a single intrinsic free energy of binding contribution is used for each rigid receptor structure.

For the receptor ensemble average, eq 3 is used with B_n calculated by either eqs 4 or 5. A dominant state approximation may also be invoked where only a single receptor configuration [min$_n$ (B$_n$)] is used.[61]

Values of $N = 50$ and $\Delta G_\xi = 0.9$ kcal mol^{-1} were employed here (see section 2.2). A maximum of $P = 20$ complex configurations were drawn from docking a ligand to each rigid receptor configuration. Thus, a maximum of 1000 binding poses were used in eq 3. For the calculation of B_E in eq 4, poses with intrinsic free energies less favorable by 2.0 kcal mol^{-1} than the most stable pose were discarded, effectively leading to $1 \leq P \leq 20$ (see Table S7).

3. RESULTS

3.1. Parametrization and Performance of LIE Models. The first goal here was to obtain an accurate yet computationally efficient free energy function to estimate the stability of a given binding pose obtained for a small-molecule and a given receptor configuration. This function was called an intrinsic binding free energy (ΔG_{int}).

Several equations based on LIE models previously proposed for implicit[41,47,49] and explicit[29,32,40,86] solvents were tested. A combination of implicit solvent and geometry optimization of

ligand−receptor complexes proved reasonably accurate and computationally fast. As indicated below by comparisons of errors observed between LIE models parametrized here and previously available, the following adapted linear interaction model for continuum electrostatics (ALICE) gave the best results

$$\Delta G_{int} \approx \Delta G_{ALICE} = k_1(2 - \eta - \pi)V^c_{vdW} + k_2(\eta + \pi)V^c_{elet} + k_3\eta(G^c_{GB} - G^p_{GB}) + k_4\pi G^l_{GB} + k_5\Delta SASA^l + k_6 \quad (6)$$

where solvent polarization free energy (G_{GB}), van der Waals (V_{vdW}), and electrostatic (V_{elet}) potentials were calculated for optimized geometries of the complex (c), protein (p), and ligand (l) species. $\Delta SASA^l$ is the difference in SASA between bound and free ligand. The processes of ligand insertion in solution and in the receptor cavity were assumed to be fully decoupled so that the 6 LIE coefficients were independent.

Energy contributions and relative polarity descriptors for ligand (π) and receptor cavity (η) are given in the Supporting Information for all ligands (Table S3 and Table S4). Parameters obtained after optimization of eq 6 against the training set described above were $k_1 = 0.09$, $k_2 = 0.31$, $k_3 = 1.16$, $k_4 = -2.85$, $k_5 = 0.017$ kcal mol^{-1} Å^{-2}, and $k_6 = 3.36$ kcal mol^{-1} (Table S6).

Binding free energies estimated with eq 6 are shown in Figure 1, Table 2, and Table S5. For the 42 small-molecule

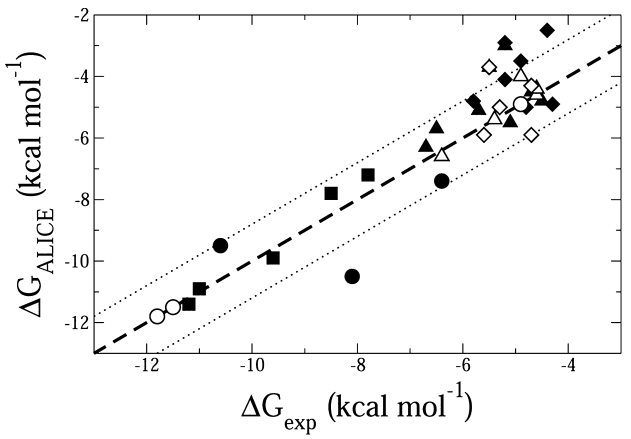

Figure 1. Binding free energies estimated by eq 6. T4 lysozyme L99A ligands are shown as triangles (▲), M102Q ligands are lozenges (◆), HIVRT ligands are circles (●), and FKBP ligands are squares (■). Ligands in the training set are shown as empty symbols, and ligands in the test set are shown as filled symbols. Dashed and dotted lines indicate $y = x \pm 1.2$ kcal mol^{-1}.

complexes in the test set, the RMSD between calculated (ΔG_{ALICE}) and experimental affinities is 1.2 kcal mol^{-1}, the coefficient of determination (R^2)[87] is 0.8, and the maximum error (E_{max}) is 3.0 kcal mol^{-1} (Table S6), which drops to 2.4 kcal mol^{-1} if only binder molecules are considered. All false-positive poses were properly recognized, but many nonbinders were not.

In order to compare the results of eq 6 with the Vina docking energy function,[21] ligands in our test set were docked with Vina to their respective protein crystal structure (native docking) or to a congeneric holo structure if a native one was not available. The binding pose given by the most favorable score in Vina was chosen for comparisons. Error analysis shows that binding free energies calculated with eq 6 resulted in smaller deviations from experiment than those estimated with Vina (RMSD = 1.1 or 1.7 kcal mol^{-1}, E_{max} = 2.2 or 4.3 kcal mol^{-1}, and R^2 = 0.7 or 0.4, respectively). In particular, the performance of our ALICE model is significantly better than Vina if only FKBP ligands are considered (RMSD = 0.6 or 2.6 kcal mol^{-1}, E_{max} = 1.0 or 4.3 kcal mol^{-1}, and R^2 = 0.8 or −2.8, respectively).

It is instructive to describe some of the other LIE models parametrized and tested here. An implicit solvent LIE equation equivalent to the formulation given by Su et al.[49] but with the cavity and van der Waals free energies of solvation condensed to one nonpolar contribution[46] (eq S1 in the SI) resulted in a RMSD of 2.2 kcal mol for the test set (E_{max} = 5.6 kcal mol^{-1}). Affinities estimated with an adaptative version of the same model (eq S2) resulted in a RMSD of 1.6 kcal mol^{-1} (E_{max} = 4.6 kcal mol^{-1}). An adapted LIE eq (eq S3) in which k_6 was scaled by $(1-\eta)$ presented a RMSD of 1.4 kcal mol^{-1} (E_{max} = 2.8 kcal mol^{-1}). The number of outliers found for predictions with this last model was, however, 50% larger than found with eq 6 (Table S6).

Adapted LIE models with the same energetic contributions but with different combinations of the polarity descriptors were also tested, but eq 6 is the most accurate model. A similar result was observed by Linder et al.[40] for adapted LIE models in explicit solvent.

3.2. Averaging Multiple Ligand and Receptor Configurations. The second goal of this study was to test procedures and approximations based on the implicit ligand theory[61] to average the intrinsic free energies calculated for an ensemble of ligand−receptor complexes. Three combinations of ligand pose and receptor configuration averages were tested: In ΔG_{EE}, eq 4 is used to average the ligand poses and to calculate the binding potential of mean-force for each receptor structure, and eq 3 is used to average the receptor configurational distribution. In ΔG_{DE}, eq 5 is used to calculate the binding potential of mean-force, and eq 3 is used to average the receptor distribution. Finally in ΔG_{DD}, eq 5 is again used to calculate the binding potential of mean-force, and a dominant state approximation is used for the receptor distribution (see section 2.5).

Table 3 shows results obtained by the averaging procedures for the full ligand set (previously divided in training and test sets). Error analysis in comparison to experimental affinities is shown in Table 4.

The highest deviations observed in Table 3 are due to the L99A ligands benzene, toluene, and 1,3,5-trimethylbenzene and to the M102Q ligands 2-fluoroaniline, toluene, 3-methylpyrrole, thieno[3.2-b]thiophene, and *N*-(*o*-tolyl)cyanoformamide. All of these also show high ΔG_{ALICE} deviations. In order to isolate contributions of the averaging procedures from inaccuracies in the intrinsic free energy function, all ALICE outliers, i.e., the ligands cited above and catechol, 2-methoxyphenol, 4-vinylpyridine, and HIV3, were removed from the error analysis.

Deviations calculated for this ligand set show slightly smaller RMSDs and determination coefficients closer to one when going from the exponential averages (ΔG_{EE}) to the dominant pose (ΔG_{DE}) and state (ΔG_{DD}) approximations. However, the maximum errors (E_{max}) are higher for ΔG_{DD} due to overstabilization of HIVRT and FKBP ligands.

It is useful to analyze errors for each receptor separately. For T4 lysozyme mutants, the dominant pose and state approximation results in smaller deviations than the exponential averaging procedures. In fact, ΔG_{DD} shows a RMSD smaller than that observed for ΔG_{ALICE} for L99A ligands (Table 2 and Table S6) suggesting that receptor conformational selection

Table 3. Binding Free Energies (in kcal mol^{-1}) Experimentally Measured and Estimated by the Averaging Procedures Described in the Text for the Full Ligand Set

ligand	ΔG_{exp}[a]	ΔG_{EE}	ΔG_{DE}	ΔG_{DD}
L99A				
isobutylbenzene	−6.4	−4.1	−4.4	−5.6
4-ethyltoluene	−5.4	−3.7	−4.1	−4.7
para-xylene	−4.6	−3.1	−3.5	−4.1
indole	−4.9	−2.7	−3.2	−3.8
ortho-xylene	−4.6	−3.1	−3.6	−4.2
n-butylbenzene	−6.7	−4.4	−4.7	−5.7
propylbenzene	−6.5	−3.8	−4.2	−5.1
ethylbenzene	−5.7	−3.1	−3.7	−4.1
toluene	−5.5	−2.5	−3.1	−3.5
benzene	−5.2	−1.7	−2.3	−3.0
3-ethyltoluene	−5.1	−3.7	−4.1	−4.8
meta-xylene	−4.7	−3.1	−3.6	−4.0
2-ethyltoluene	−4.5	−3.7	−4.1	−4.8
3-methylpyrrole	>−2.0	−1.3	−2.0	−2.3
phenol	>−2.0	−1.5	−2.1	−2.6
1,3,5-trimethylbenzene	>−2.0	−3.6	−3.9	−4.9
cyclohexane	>−2.0	−1.9	−2.4	−2.7
2-fluoroaniline	>−2.0	−1.7	−2.3	−2.8
M102Q				
2-fluoroaniline	−5.5	−1.5	−2.1	−2.8
5-chloro-2-methylphenol	−5.3	−2.6	−3.2	−4.0
benzyl acetate	−4.7	−4.4	−4.5	−5.6
ortho-cresol	−4.7	−2.1	−2.6	−3.2
2-propylphenol	−5.6	−3.5	−3.8	−4.7
(phenylamino)acetonitrile	−5.8	−3.2	−3.4	−4.4
toluene	−5.2	−2.3	−2.6	−3.1
3-methylpyrrole	−5.2	−0.9	−1.6	−2.0
thieno[3.2-b]thiophene	−4.9	−1.7	−1.9	−2.7
2-ethylphenol	−4.8	−2.7	−3.2	−3.9
catechol	−4.4	−2.8	−3.0	−4.5
2-ethoxyphenol	−4.3	−2.6	−3.1	−3.9
phenylhydrazine	>−2.0	−1.6	−2.3	−3.2
2-methoxyphenol	>−2.0	−2.1	−2.7	−3.3
4-vinylpyridine	>−2.0	−2.3	−2.7	−3.2
N-(*o*-tolyl)cyanoformamide	>−2.0	−1.8	−2.4	−3.6
HIVRT				
HIV1	−11.5	−10.4	−11.1	−12.2
HIV2	−4.9	−4.6	−5.2	−6.3
HIV3	−8.1	−8.6	−9.2	−10.0
HIV4	−10.6	−8.7	−9.2	−10.6
HIV5	−6.4	−7.5	−8.2	−9.8
HIV6	−11.8	−10.3	−10.5	−12.0
FKBP				
FKB1	−11.0	−11.9	−12.6	−13.8
FKB2	−11.2	−11.7	−12.2	−13.3
FKB3	−7.8	−7.4	−8.2	−9.3
FKB4	−8.5	−7.6	−8.2	−9.4
FKB5	−9.6	−10.7	−11.2	−12.8

[a]Repeated from Table S3. Nonbinders were assumed to have ΔG_{exp} > −2.0 kcal mol^{-1}.

Table 4. Error Analysis of the Binding Free Energies Calculated by the Averaging Procedures Proposed for Different Ligand Sets

	ΔG_{EE}	ΔG_{DE}	ΔG_{DD}
Full Ligand Set (Table 3)[a]			
RMSD	1.7	1.5	1.3
E_{max}	2.9	2.6	3.4
R^2	0.6	0.7	0.8
L99A Ligands[a]			
RMSD	1.7	1.4	0.7
E_{max}	2.7	2.3	1.5
R^2	0.0	0.3	0.8
M102Q Ligands[a]			
RMSD	2.2	1.8	1.3
E_{max}	2.9	2.6	2.1
R^2	−3.0	−1.8	−0.4
HIVRT Ligands			
RMSD	1.2	1.2	1.7
E_{max}	1.9	1.8	3.4
R^2	0.8	0.8	0.6
FKBP Ligands			
RMSD	0.8	1.1	2.3
E_{max}	1.1	1.7	3.2
R^2	0.6	0.3	−1.9

[a]Ligands with a ΔG_{ALICE} deviation from the experimental affinity higher than one RMSD (1.2 kcal mol^{-1}, Table 2) were removed from the error analysis. Deviations (in kcal mol^{-1}, except for R^2) were calculated for each set in comparison to experimental affinities.

contributes to the calculation of binding free energies even for the small and hydrophobic L99A ligands and for the relatively rigid T4 lysozyme engineered cavity. Results for the M102Q mutant show higher deviations which in part may be due to the higher inaccuracies in the ALICE model for this receptor (Table 2).

For HIVRT and specially for FKBP ligands, the opposite trend is observed. The best predictions were obtained for exponential averaging of both pose and receptor configurations (ΔG_{EE}). The dominant approximations overstabilize the binding free energies because some binding poses are as much as 3.5 kcal mol^{-1} more stable than the experimental free energy.

The relative rankings of binding affinities among the HIVRT and the FKBP ligands are recovered with all averaging procedures, except for the two ligands with the most favorable affinities in each receptor. However, experimental and calculated differences between these two ligands are smaller than 0.3 kcal mol^{-1}.

If the Vina docking energy function is used to approximate Ψ in eq 2, the free energies predicted show significative disagreement with experiment for all ligand sets. For example, ΔG_{EE}^{Vina} calculated for the FKBP ligands give RMSD = 3.8 kcal mol^{-1}, E_{max} = 4.6 kcal mol^{-1}, and R^2 = −7.0 suggesting that the docking energy function will give meaningless results if used to approximate the solvent-mediated interaction energy in eq 2. This result can be traced to the Vina inability to discriminate false-positive poses. Almost all poses generated from docking were on average used to calculate B_E^{Vina}. On the other hand, less than half of the generated poses were on average used to calculate B_E^{ALICE} for the same set of ligand−receptor poses (Figure S2 and Table S7).

4. DISCUSSION

4.1. ALICE Model Contributions, Performance, and Limitations. Several LIE equations with different definitions of the nonpolar solvation contribution and with different combinations of polarity descriptors were described and tested here. The best predictions for a test set composed of 42 small-

molecule complexes of 4 different receptors were obtained with eq 6 with 6 adjustable parameters. None of the ligands in the test set were used in the parametrization training set. Deviations observed with this ALICE model and with previously proposed LIE models are similar. For instance, the implicit solvent LIE model proposed by Su et al. has 4 adjustable parameters and resulted in a RMSD of 1.3 kcal mol^{-1} with R^2 = 0.62 for a set of 57 HIVRT ligands (including the 6 HIVRT ligands used here).[49] The implicit solvent LIE model with 2 adjustable parameters proposed by Kolb et al. showed a RMSD of 1.6 kcal mol^{-1} with a correlation coefficient of 0.52 for a set of 128 EGFR kinase ligands.[36] The LIE model proposed by Wall et al. has 3 adjustable parameters and showed a RMSD of 1.6 kcal mol^{-1} and a correlation coefficient of 0.62 for a set of 15 neuraminidase inhibitors.[35] Finally, the adapted LIE model for explicit solvent proposed by Linder et al. has 3 adjustable parameters and resulted in a mean absolute deviation (similar to a RMSD) of 1.6 kcal mol^{-1}, E_{max} = 3.4 kcal mol^{-1}, and R^2 = 0.72 for a diverse set of 38 ligands and their respective 16 receptors.[40] Deviations reported for these four LIE models were obtained with the same ligands (or with a congeneric set of ligands) used for training the models. Still, the ALICE model proposed has the smallest RMSD and the determination coefficient closest to 1.

In order to analyze the energy contributions included in the ALICE model, it should be noted that implicit solvation is not pairwise decomposable in general. Consequently, the splitting of solute−solvent interactions necessary for LIE calculations is not unique. The solvent polarization energy in the bound ligand state is given by $(G^{c}_{GB} - G^{c'}_{GB})$ where the initial state, c', indicates a complex with ligand charges turned off. As discussed by Su et al.,[49] the initial state is approximated here to the free protein (p). With the GBr^6 method,[43] the electrostatic polarization energy calculated for the training set changes by 0.2−0.7 kcal mol^{-1} between these two initial state definitions. This polarization response is scaled by the cavity polarity descriptor in eq 6. A combination with the ligand polarity did not result in better predictions.

Nonpolar solvent contributions from the free ligand and the receptor complex were replaced by a simple $\Delta SASA$ term without loss of accuracy. Previous work suggested that the constant term in a LIE equation, γ in eq 1 or k_6 in eq 6, may be related to binding site hydrophobicity[32,34] or nonpolar surface area.[88] An ALICE model (eq S3 in the SI) in which the constant term is scaled by the nonpolar cavity surface $(1-\eta)$ was tested, but this modification also did not result in better performance.

The comparable accuracy obtained here for different LIE models (eq 6 and eqs S1−S3) suggests the exact form of a LIE equation is less important given a proper parametrization is conducted. Significant departure from theoretical values is observed for the parameters obtained here. For instance, $k_2(\eta+\pi)$, equivalent to the parameter β in previous LIE models (eq 1), ranged from 0.03 to 0.27. This is below the theoretical value of β = 0.5.[29,49] It is expected that parameter values will mutually compensate model assumptions and inaccuracies in the solvent model, molecular mechanical potentials, etc. Thus, the parametrized LIE equations presented here may be cast as linear free energy relationships which coefficients are only bounded by the linear response theory.[30]

Applications of these LIE models depend, however, on their transferability for receptors and ligands not included in the training set used to parametrize the equations. Here coefficients were scaled by ligand and cavity polarities in order to increase model transferability.[40] Eq 6 correctly predicts affinities for ligands which receptors were either included (T4 lysozyme and HIVRT) or not (FKBP) in the training set. The sensitivity of ΔG_{ALICE} on the η and π descriptor values is small. Variations of ∼0.2 kcal mol^{-1} were observed when descriptor values were scaled by ±20%. Predictions for other receptors and ligands should have similar accuracy, but an extensive test of transferability is left for future studies.

The computational efficiency observed for eq 6 suggests it can be used to predict affinities for large ligand sets. For instance, our ALICE model could be used instead of the scoring or energy functions currently employed in molecular docking. To this end, ligand−receptor poses would have to be generated by the conformational search procedures found in docking[21,50] or by another method such as mining-minima.[89] Ligand and protein topologies containing connectivity, force field parameters, and polarity descriptors would have to be available or built. Although cumbersome when manually done, this process can be made fairly automatic.[64,66,90]

In order to improve the ALICE model proposed, it may be useful to analyze the highest deviations found. The following ligands are described as eq 6 outliers since they show deviations larger than one RMSD: benzene, toluene, 1,3,5-trimethylbenzene (L99A), 2-fluoroaniline, catechol, 3-methylpyrrole, thieno[3,2-*b*]thiophene, 4-vinylpiridine, 2-methoxyphenol, *N*-(*o*-tolyl)cyanoformamide (M102Q), and HIV3. All but 2-fluoroaniline belong to the test set, and all T4 lysozyme outliers have underestimated free energies. Most of these ligands are also outliers for eqs S1−S3 (see Table S6).

The binding affinity increases for L99A ligands upon addition of linear methylene units, as seen for benzene to toluene and up to *n*-butylbenzene. The experimental free energy difference upon methylene addition in this series is 0.2−0.3 kcal mol^{-1} but between ethylbenzene and propylbenzene, which is 0.8 kcal mol^{-1}. Although eq 6 incorrectly predicts a small stability to benzene and toluene, appropriate affinities are predicted upon increasing the number of methylene units. This observation suggests a slightly unbalanced description of the nonpolar contributions involving aliphatic and aromatic carbons. An atom-type dependent surface tension, k_5 in eq 6, could amend this problem.

The hydrophobic ligand 1,3,5-trimethylbenzene should interact more favorably with the L99A nonpolar engineered binding site than with water, as suggested by the free energy calculated with the ALICE model. Docking suggests that there is enough room to accommodate this relatively bulky ligand in the L99A cavity (Table S7). However, the experimental free energy shows that 1,3,5-trimethylbenzene is a L99A nonbinder. As T4 lysozyme must show some breathing or opening movement to allow the entrance or exit of ligands from the engineered cavity,[91] we speculate that 1,3,5-trimethylbenzene is a kinetic nonbinder and that there may not be a low energy pathway allowing its entrance into the L99A cavity.

The highest number of outliers were found for M102Q ligands. Possibly electrostatic interactions were not described or sampled correctly in the LIE models tested. Yet no correlation was found between outliers and significant flaws in the description of their dipole moments (Table S1) or the availability of experimental ligand−receptor structures. The lack of holo crystal structures for some ligands and the possibility that receptor structures used for the calculation of ΔG_{ALICE} are not representative of complexes observed in

aqueous solution may contribute for inaccuracies in the prediction of intrinsic binding free energies. This appears to be the case for catechol as discussed in the next section.

4.2. Analysis of the Proposed Conformational Averaging Schemes. Ensembles for all target receptors were initially built with apo protein representations. For the T4 lysozyme mutants, 3 structures out of 50 in the L99A ensemble and 11 structures out of 50 for the M102Q ensemble had their binding cavity fully blocked by side-chains rotations. Docking to these receptor structures did not yield complexes with ligand inside the engineered binding site even for small ligands such as toluene. This problem was more pronounced for the HIVRT and FKBP bulky ligands as none of the receptor structures obtained from apo molecular dynamics after equilibration were able to accommodate ligands in its crystallographic binding site. Thus, molecular dynamics obtained from holo structures were used to generate the HIVRT and FKBP ensembles.

Affinities were consistently underestimated for T4 lysozyme mutants by all three combinations of ensemble averages tested. Although ΔG_{DD} shows a small RMSD and a favorable error analysis for L99A ligands, the dominant approximation that counts only the most favorable pose underestimates affinities for almost all T4 lysozyme ligands but catechol (see below). This tendency suggests that the tentative apo M102Q ensemble used here systematically degrades the structural representation in comparison to the crystal structures. As noted, side-chains rotations block the binding cavity even for the relatively rigid engineered site in T4 lysozyme. Apo protein ensembles have to be used carefully and possibly enlarged or modified[92] to accommodate ligand binding.

The only notable exception is catechol binding to M102Q. Although the ALICE free energy function predicts unstable binding for catechol to the crystal (holo) configuration, favorable binding is predicted by ΔG_{DD}. Thus, receptor configurational sampling is important for the prediction of catechol binding, and the M102Q crystal configuration may have a low contribution to the binding affinity. In fact, it has been shown that catechol has at least two binding modes[93] and that enhanced sampling is required to compute its binding free energy correctly.[18]

Increasing the number of poses that contribute to exponential averaging results in less favorable binding free energies for all ligands tested. This "dilution" effect has two possible causes. One is artificially related to the discrimination of poses that should contribute to the ensemble averages. It depends on the discriminatory quality of the intrinsic free energy function. The second cause has a physical origin as the macroscopically measured affinity may be an average of several binding poses, some of which will have higher intrinsic free energies of binding.

Free energies calculated for the T4 lysozyme mutants decrease up to 50% on going from ΔG_{DD} to ΔG_{EE}. The dilution effect is more pronounced for T4 lysozyme because the intrinsic free energy differences between ligand poses inside or outside the engineered binding site is small (<2.0 kcal mol^{-1}). Consequently, it is harder to discriminate poses that should contribute to the ensemble averages from decoy poses. In fact, for all T4 lysozyme ligands, the average number of poses included in the calculation of the binding potential of mean-force (eq 4) is higher than the average number of poses inside the receptor binding site (Table S7).

The importance of pose discrimination on ensemble averages is also illustrated when the Vina energy function is used as an approximation instead of ΔG_{ALICE} (eq 6). The exponentially averaged free energies obtained in this case are significantly less favorable than the corresponding dominant approximation (ΔG_{DD}^{Vina}) for the same set of ligand−receptor poses.

For HIVRT and FKBP ligands, pose discrimination with the ALICE model is rather accurate. Although the absolute values of binding free energies are higher, the predictions with the ALICE intrinsic free energy function show smaller deviations for both receptors (Table 2). The better discrimination is reflected by the average number of poses used to calculate B_E which is closer to the average number of poses found inside the receptor binding site (Table S7).

Thus, for HIVRT and FKBP ligands, the decrease of calculated free energies on going from ΔG_{DD} to ΔG_{EE} does not appear artifactual but a physical effect due to averaging a distribution of ligand−receptor conformations. Induced fit is expected to change the receptor conformational distribution upon ligand complexation. Indeed, some of the configurations found for the complexes with the receptor ensemble show more favorable intrinsic free energies of binding. This also explains the overstabilization observed for ΔG_{DD} predictions.

Receptor reorganization free energy will be accounted for if the ensemble is canonically distributed and wide enough to represent the relevant receptor motions. If ligand binding has a large reorganization free energy, the associated receptor motions will have high free energy costs, and the number or fraction of binding-competent configurations in the ensemble will be small. Consequently, a ligand complex formed with such rare receptor configurations will only contribute significatively to the final exponential average if it has a highly favorable intrinsic binding free energy. On the other hand, if the reorganization free energy for ligand binding is small, the fraction of binding-competent configurations in the ensemble will be large, and a reasonable number of ligand complexes with these popular receptor configurations will contribute to the average even if their intrinsic binding free energies are not highly favorable.

We do not investigate here what is the appropriate size of the ensemble to account for the reorganization energy correctly, but 50 configurations appear to be insufficient, specially if an apo structure is used to generate the ensemble.[92] When a holo structure is used to generate a tentative ensemble, the full receptor reorganization energy may not be accounted for, but the relative contribution upon a series of congeneric ligands can be retrieved.

Finally, which of the three averaging procedures should be applied? The answer depends on the receptor ensemble and the intrinsic free energy function. For receptor ensembles with unknown or biased distributions, with insufficient sampling and for free energy functions that cannot discriminate correct binding poses from decoys, the dominant pose and state approximation (ΔG_{DD}) should be applied. For more flexible receptors and upon increasing the quality of the conformational ensemble, the state exponential average (ΔG_{DE}) might be included. The exponential average for multiple ligand configurations (ΔG_{EE}) should be employed only when a calibrated and discriminatory intrinsic free energy function is available. This is probably the case for the ALICE model proposed (eq 6) with lead-like ligands.

5. CONCLUSIONS

We have parametrized an adapted linear interaction energy model that employs a simple combination of energy

minimization of ligand-protein geometries with implicit solvation. This model is able to retrospectively predict binding affinities for different receptors with accuracy similar to other LIE models which employ more expensive molecular dynamics simulations to sample configurations and more detailed solvent models.[29−31,40,49] LIE models using geometry optimization and implicit solvation have already been successfully applied by other authors.[36,47]

Conformational sampling is divided and approximated in several steps here. Solvent degrees of freedom, in particular the important dielectric response, are treated implicitly with a continuum electrostatic model. Ligand internal torsion and relative orientation in receptor complexes are evaluated within the docking algorithm when poses are generated. Finally, receptor conformations are sampled from a configurational ensemble, which is generated once and repeatedly used for preparing ligand-protein complexes for a series of congeneric ligands. It should be noted that the proposed ALICE model can be used to predict binding affinities given either a single receptor structure or a conformational distribution.

For the prediction of binding to flexible protein targets, it is useful to represent the receptor structure by conformational ensembles.[6,7,53,56,57] Based on the implicit ligand theory,[61] averaging procedures were proposed and tested to estimate affinities for ligand binding to four different receptors with structures represented by tentative conformational ensembles. The scheme proposed is computationally efficient and could be applied to average contributions of $\sim 10^6$ ligand−receptor poses for each ligand tested.

In principle, to be useful in the prediction of ligand binding, a receptor conformational ensemble should follow the Boltzmann distribution and describe all motions or structural rearrangements relevant for small-molecule complexation. Here, tentative ensembles were built without much attention to statistical distribution or to sampling of relevant motions by running simple molecular dynamics in implicit solvent. Consequently, results obtained by averaging contributions from these receptor ensembles do not aim to reproduce experimental affinities and should be analyzed only qualitatively. It should be noted that there is no consensus on how to obtain conformational ensembles that are suitable to predict ligand binding.[7,53,54,92]

Nevertheless, we find that good discrimination between binding poses and decoys is essential to calculate accurate binding affinities, particularly when contributions from several putative binding poses and different receptor configurations are (exponentially) averaged. Approximations used here such as sampling by docking instead of a statistical distribution or innacuracies in the intrinsic free energy function may contribute to the difficulty in distinguishing binding poses from decoys. For lead-like ligands, we found that the ALICE model proposed is able to discriminate poses resulting in binding free energy predictions in good agreement with experiment.

■ ASSOCIATED CONTENT

Supporting Information

Equations S1−S3, figures with HIVRT and FKBP ligand structures and an example of ligand pose distribution for T4 lysozyme, and tables with dipole moments, number of torsions activated in docking, experimental energies, descriptors and LIE contributions for all ligands considered, training set predictions, error analysis, and number of poses used in averaging procedures. This material is available free of charge via the Internet at http://pubs.acs.org.

■ AUTHOR INFORMATION

Corresponding Author

*E-mail:garantes@iq.usp.br.

Notes

The authors declare no competing financial interest.

■ ACKNOWLEDGMENTS

Funding from FAPESP (projects 11/04354-6 and 12/02501-4) and CNPq (project 141950/2013-7) are gratefully acknowledged.

■ REFERENCES

(1) Jorgensen, W. L. The Many Roles of Computation in Drug Discovery. *Science* **2004**, *303*, 1813−1818.
(2) Ballester, P. J.; Schreyer, A.; Blundell, T. L. Does a More Precise Chemical Description of Protein−Ligand Complexes Lead to More Accurate Prediction of Binding Affinity? *J. Chem. Inf. Model.* **2014**, *54*, 944−955.
(3) Fleishman, S.; Baker, D. Role of the Biomolecular Energy Gap in Protein Design, Structure, and Evolution. *Cell* **2012**, *149*, 262−273.
(4) Faver, J. C.; Yang, W.; Merz, K. M. The Effects of Computational Modeling Errors on the Estimation of Statistical Mechanical Variables. *J. Chem. Theory Comput.* **2012**, *8*, 3769−3776.
(5) Zuckerman, D. M. Equilibrium Sampling in Biomolecular Simulations. *Annu. Rev. Biophys.* **2011**, *40*, 41−62.
(6) Benedix, A.; Becker, C. M.; de Groot, B. L.; Caflisch, A.; Bockmann, R. A. Predicting Free Energy Changes Using Structural Ensembles. *Nat. Methods* **2009**, *6*, 3−4.
(7) Arantes, G. M. Flexibility and Inhibitor Binding in Cdc25 Phosphatases. *Proteins* **2010**, *78*, 3017−3032.
(8) Gilson, M. K.; Zhou, H. X. Calculation of Protein−Ligand Binding Affinities. *Annu. Rev. Biophys. Biomol. Struct.* **2007**, *36*, 21−42.
(9) Guvench, O.; MacKerell, A. D., Jr. Computational Evaluation of Protein−Small Molecule Binding. *Curr. Opin. Struct. Biol.* **2009**, *19*, 56−61.
(10) Deng, Y.; Roux, B. Computations of Standard Binding Free Energies with Molecular Dynamics Simulations. *J. Phys. Chem. B* **2009**, *113*, 2234−2246.
(11) Christ, C. D.; Mark, A. E.; van Gunsteren, W. F. Basic Ingredients of Free Energy Calculations: a Review. *J. Comput. Chem.* **2010**, *31*, 1569−1582.
(12) Gallicchio, E.; Levy, R. M. Advances in All Atom Sampling Methods for Modeling Protein−Ligand Binding Affinities. *Curr. Opin. Struct. Biol.* **2011**, *21*, 161−166.
(13) Chodera, J. D.; Mobley, D. L.; Shirts, M. R.; Dixon, R. W.; Branson, K.; Pande, V. S. Alchemical Free Energy Methods for Drug Discovery: Progress and Challenges. *Curr. Opin. Struct. Biol.* **2011**, *21*, 150−160.
(14) Rizzo, R. C.; Tirado-Rives, J.; Jorgensen, W. L. Estimation of Binding Affinities for HEPT and Nevirapine Analogues with HIV−1 Reverse Transcriptase Via Monte Carlo Simulations. *J. Med. Chem.* **2001**, *44*, 145−154.
(15) Mobley, D. L.; Graves, A. P.; Chodera, J. D.; McReynolds, A. C.; Shoichet, B. K.; Dill, K. A. Predicting Absolute Ligand Binding Free Energies to a Simple Model Site. *J. Mol. Biol.* **2007**, *371*, 1118−1134.
(16) Jayachandran, G.; Shirts, M. R.; Park, S.; Pande, V. S. Parallelized−Over−Parts Computation of Absolute Binding Free Energy with Docking and Molecular Dynamics. *J. Chem. Phys.* **2006**, *125*, 084901.
(17) Boyce, S. E.; Mobley, D. L.; Rocklin, G. J.; Graves, A. P.; Dill, K. A.; Shoichet, B. K. Predicting Ligand Binding Affinity with Alchemical Free Energy Methods in a Polar Model Binding Site. *J. Mol. Biol.* **2009**, *394*, 747−763.

(18) Mobley, D. L.; Chodera, J. D.; Dill, K. A. On the Use of Orientational Restraints and Symmetry Corrections in Alchemical Free Energy Calculations. *J. Chem. Phys.* **2006**, *125*, 084902.
(19) Kuntz, I. D.; Blaney, J. M.; Oatley, S. J.; Langridge, R.; Ferrin, T. E. A Geometric Approach to Macromolecule−Ligand Interactions. *J. Mol. Biol.* **1982**, *161*, 269−288.
(20) Sousa, S. F.; Fernandes, P. A.; Ramos, M. J. Protein−Ligand Docking: Current Status and Future Challenges. *Proteins* **2006**, *65*, 15−26.
(21) Trott, O.; Olson, A. J. AutoDock Vina: Improving the Speed and Accuracy of Docking with a New Scoring Function, Efficient Optimization, and Multithreading. *J. Comput. Chem.* **2010**, *31*, 455−461.
(22) Bowman, A. L.; Nikolovska-Coleska, Z.; Zhong, H.; Wang, S.; Carlson, H. A. Small Molecule Inhibitors of the MDM2−P53 Interaction Discovered by Ensemble−Based Receptor Models. *J. Am. Chem. Soc.* **2007**, *129*, 12809−12814.
(23) Plewczynski, D.; Lazniewski, M.; Augustyniak, R.; Ginalski, K. Can We Trust Docking Results? Evaluation of Seven Commonly Used Programs on PDBbind Database. *J. Comput. Chem.* **2011**, *32*, 742−755.
(24) Keenan, S. M.; Geyer, J. A.; Welsh, W. J.; Prigge, S. T.; Waters, N. C. Rational Inhibitor Design and Iterative Screening in the Identification of Selective Plasmodial Cyclin Dependent Kinase Inhibitors. *Comb. Chem. High Throughput Screening* **2005**, *8*, 27−38.
(25) Bisson, W. H.; Cheltsov, A. V.; Bruey-Sedano, N.; Lin, B.; Chen, J.; Goldberger, N.; May, L. T.; Christopoulos, A.; Dalton, J. T.; Sexton, P. M.; Zhang, X.-K.; Abagyan, R. Discovery of Antiandrogen Activity of Nonsteroidal Scaffolds of Marketed Drugs. *Proc. Natl. Acad. Sci. U. S. A.* **2007**, *104*, 11927−11932.
(26) Frimurer, T. M.; Peters, G. H.; Iversen, L. F.; Andersen, H. S.; Møller, N. P. H.; Olsen, O. H. Ligand−Induced Conformational Changes: Improved Predictions of Ligand Binding Conformations and Affinities. *Biophys. J.* **2003**, *84*, 2273−2281.
(27) Kitchen, D. B.; Decornez, H.; Furr, J. R.; Bajorath, J. Docking and Scoring in Virtual Screening for Drug Discovery: Methods and Applications. *Nat. Rev. Drug Discovery* **2004**, *3*, 935−949.
(28) Kim, R.; Skolnick, J. Assessment of Programs for Ligand Binding Affinity Prediction. *J. Comput. Chem.* **2008**, *29*, 1316−1331.
(29) Åqvist, J.; Medina, C.; Sammuelsson, J.-E. A New Method for Predicting Binding Affinity in Computer−Aided Drug Design. *Protein Eng.* **1994**, *7*, 385−391.
(30) Carlson, H. A.; Jorgensen, W. L. An Extended Linear Response Method for Determining Free Energies of Hydration. *J. Phys. Chem.* **1995**, *99*, 10667−10673.
(31) Gallicchio, E.; Kubo, M. M.; Levy, R. M. Enthalpy−Entropy and Cavity Decomposition of Alkane Hydration Free Energies: Numerical Results and Implications for Theories of Hydrophobic Solvation. *J. Phys. Chem. B* **2000**, *104*, 6271−6285.
(32) Åqvist, J.; Luzhkov, V. B.; Brandsdal, B. O. Ligand Binding Affinities from MD Simulations. *Acc. Chem. Res.* **2002**, *35*, 358−365.
(33) King, G.; Warshel, A. Investigation of the Free Energy Functions for Electron Transfer Reactions. *J. Chem. Phys.* **1990**, *93*, 8682−8692.
(34) Almlof, M.; Brandsdal, B. O.; Åqvist, J. Binding Affinity Prediction with Different Force Fields: Examination of the Linear Interaction Energy Method. *J. Comput. Chem.* **2004**, *25*, 1242−1254.
(35) Wall, I. D.; Leach, A. R.; Salt, D. W.; Ford, M. G.; Essex, J. W. Binding Constants of Neuraminidase Inhibitors: an Investigation of the Linear Interaction Energy Method. *J. Med. Chem.* **1999**, *42*, 5142−5152.
(36) Kolb, P.; Huang, D.; Dey, F.; Caflisch, A. Discovery of Kinase Inhibitors by High−Throughput Docking and Scoring Based on a Transferable Linear Interaction Energy Model. *J. Med. Chem.* **2008**, *51*, 1179−1188.
(37) Stjernschantz, E.; Marelius, J.; Medina, C.; Jacobsson, M.; Vermeulen, N. P. E.; Oostenbrink, C. Are Automated Molecular Dynamics Simulations and Binding Free Energy Calculations Realistic Tools in Lead Optimization? An Evaluation of the Linear Interaction Energy (LIE) Method. *J. Chem. Inf. Model.* **2006**, *46*, 1972−1983.
(38) de Amorim, H. L. N.; Caceres, R. A.; Netz, P. A. Linear Interaction Energy (LIE) Method in Lead Discovery and Optimization. *Curr. Drug Targets* **2008**, *9*, 1100−1105.
(39) Hansson, T.; Marelius, J.; Åqvist, J. Ligand Binding Affinity Prediction by Linear Interaction Energy Methods. *J. Comput.-Aided Mol. Des.* **1998**, *12*, 27−35.
(40) Linder, M.; Ranganathan, A.; Brinck, T. Adapted Linear Interaction Energy": a Structure−Based LIE Parametrization for Fast Prediction of Protein−Ligand Affinities. *J. Chem. Theory Comput.* **2013**, *9*, 1230−1239.
(41) Zhou, R. H.; Friesner, R. A.; Ghosh, A.; Rizzo, R. C.; Jorgensen, W. L.; Levy, R. M. New Linear Interaction Method for Binding Affinity Calculations Using a Continuum Solvent Model. *J. Phys. Chem. B* **2001**, *105*, 10388−10397.
(42) Alves, A. F. N. M.Sc. thesis, Instituto de Química, Universidade de São Paulo, São Paulo, 2013. Available at http://www.teses.usp.br/teses/disponiveis/46/46131/tde-08052013-144801/ (accessed June 20, 2014).
(43) Tjong, H.; Zhou, H.-X. GBr^6: A Parameterization−Free, Accurate, Analytical Generalized Born Method. *J. Phys. Chem. B* **2007**, *111*, 3055−3061.
(44) Still, W. C.; Tempczyk, A.; Hawley, R. C.; Hendrickson, T. Semianalytical Treatment of Solvation for Molecular Mechanics and Dynamics. *J. Am. Chem. Soc.* **1990**, *112*, 6127−6129.
(45) Onufriev, A.; Bashford, D.; Case, D. A. Exploring Protein Native States and Large−Scale Conformational Changes with a Modified Generalized Born Model. *Proteins* **2004**, *55*, 383−394.
(46) Schaefer, M.; Bartels, C.; Karplus, M. Solution Conformations and Thermodynamics of Structured Peptides: Molecular Dynamics Simulation with an Implicit Solvation Model. *J. Mol. Biol.* **1998**, *284*, 835−848.
(47) Huang, D.; Caflisch, A. Efficient Evaluation of Binding Free Energy Using Continuum Electrostatic Solvation. *J. Med. Chem.* **2004**, *47*, 5791−5797.
(48) Carlsson, J.; Ander, M.; Nervall, M.; Åqvist, J. Continuum Solvation Models in the Linear Interaction Energy Method. *J. Phys. Chem. B* **2006**, *110*, 12034−12041.
(49) Su, Y.; Gallicchio, E.; Das, K.; Arnold, E.; Levy, R. M. Linear Interaction Energy (LIE) Models for Ligand Binding in Implicit Solvent: Theory and Application to the Binding of NNRTIs to HIV−1 Reverse Transcriptase. *J. Chem. Theory Comput.* **2007**, *3*, 256−277.
(50) Huey, R.; Morris, G. M.; Olson, A. J.; Goodsell, D. S. A Semiempirical Free Energy Force Field with Charge−Based Desolvation. *J. Comput. Chem.* **2007**, *28*, 1145−1152.
(51) Cavasotto, C. N.; Abagyan, R. A. Protein Flexibility in Ligand Docking and Virtual Screening to Protein Kinases. *J. Mol. Biol.* **2004**, *337*, 209−225.
(52) Erickson, J. A.; Jalaie, M.; Robertson, D. H.; Lewis, R. A.; Vieth, M. Lessons in Molecular Recognition: the Effects of Ligand and Protein Flexibility on Molecular Docking Accuracy. *J. Med. Chem.* **2004**, *47*, 45−55.
(53) Wong, C. F.; Kua, J.; Zhang, Y.; Straatsma, T.; McCammon, J. A. Molecular Docking of Balanol to Dynamics Snapshots of Protein Kinase A. *Proteins* **2005**, *61*, 850−858.
(54) Mamonov, A. B.; Bhatt, D.; Cashman, D. J.; Ding, Y.; Zuckerman, D. M. General Library−Based Monte Carlo Technique Enables Equilibrium Sampling of Semi−Atomistic Protein Models. *J. Phys. Chem. B* **2009**, *113*, 10891−10904.
(55) Kallblad, P.; Mancera, R. L.; Todorov, N. P. Assessment of Multiple Binding Modes in Ligand−Protein Docking. *J. Med. Chem.* **2004**, *47*, 3334−3337.
(56) Novoa, E. M.; de Pouplana, L. R.; Barril, X.; Orozco, M. Ensemble Docking from Homology Models. *J. Chem. Theory Comput.* **2010**, *6*, 2547−2557.
(57) Totrov, M.; Abagyan, R. Flexible Ligand Docking to Multiple Receptor Conformations: A Practical Alternative. *Curr. Opin. Struct. Biol.* **2008**, *18*, 178−184.

(58) B-Rao, C.; Subramanian, J.; Sharma, S. D. Managing Protein Flexibility in Docking and Its Applications. *Drug Discovery Today* **2009**, *14*, 394−400.
(59) Cozzini, P.; Kellogg, G. E.; Spyrakis, F.; Abraham, D. J.; Costantino, G.; Emerson, A.; Fanelli, F.; Gohlke, H.; Kuhn, L. A.; Morris, G. M.; Orozco, M.; Pertinhez, T. A.; Rizzi, M.; Sotriffer, C. A. Target Flexibility: an Emerging Consideration in Drug Discovery and Design. *J. Med. Chem.* **2008**, *51*, 6237−6255.
(60) Gallicchio, E.; Lapelosa, M.; Levy, R. M. Binding Energy Distribution Analysis Method (BEDAM) for Estimation of Protein−Ligand Binding Affinities. *J. Chem. Theory Comput.* **2010**, *6*, 2961−2977.
(61) Minh, D. D. L. Implicit Ligand Theory: Rigorous Binding Free Energies and Thermodynamic Expectations from Molecular Docking. *J. Chem. Phys.* **2012**, *137*, 104106.
(62) Eriksson, A. E.; Baase, W. A.; Wozniak, J. A.; Matthews, B. W. A Cavity−Containing Mutant of T4 Lysozyme Is Stabilized by Buried Benzene. *Nature* **1992**, *355*, 371−373.
(63) Wei, B. Q.; Baase, W. A.; Weaver, L. H.; Matthews, B. W.; Shoichet, B. K. A Model Binding Site for Testing Scoring Functions in Molecular Docking. *J. Mol. Biol.* **2002**, *322*, 339−355.
(64) Voss, N. R.; Gerstein, M.; Steitz, T. A.; Moore, P. B. The Geometry of the Ribosomal Polypeptide Exit Tunnel. *J. Mol. Biol.* **2006**, *360*, 893−906.
(65) Ertl, P.; Rohde, B.; Selzer, P. Fast Calculation of Molecular Polar Surface Area As a Sum of Fragment−Based Contributions and Its Application to the Prediction of Drug Transport Properties. *J. Med. Chem.* **2000**, *43*, 3714−3717.
(66) Hendlich, M.; Bergner, A.; Gunther, J.; Klebe, G. Relibase: Design and Development of a Database for Comprehensive Analysis of Protein−Ligand Interactions. *J. Mol. Biol.* **2003**, *326*, 607−620.
(67) Carroll, D. L. *Genetic Algorithm Driver, Version 1.7*; 1998.
(68) Press, W. H.; Teukolsky, S. A.; Vetterling, W. T.; Flannery, B. P. *Numerical Recipes in FORTRAN 77: the Art of Scientific Computing*, 2nd ed.; Cambridge University Press: Cambridge, 1992.
(69) Arantes, G. M.; Loos, M. Specific Parametrisation of a Hybrid Potential to Simulate Reactions in Phosphatases. *Phys. Chem. Chem. Phys.* **2006**, *8*, 347−353.
(70) Chinea, G.; Padron, G.; Hooft, R. W. W.; Sander, C.; Vriend, G. The Use of Position−Specific Rotamers in Model−Building by Homology. *Proteins* **1995**, *23*, 415−421.
(71) Pronk, S.; Pall, S.; Schulz, R.; Larsson, P.; Bjelkmar, P.; Apostolov, R.; Shirts, M. R.; Smith, J. C.; Kasson, P. M.; van der Spoel, D.; Hess, B.; Lindahl, E. GROMACS 4.5: a High−Throughput and Highly Parallel Open Source Molecular Simulation Toolkit. *Bioinformatics* **2013**, *29*, 845−854.
(72) O'Boyle, N. M.; Banck, M.; James, C. A.; Morley, C.; Vandermeersch, T.; Hutchison, G. R. Open Babel: an Open Chemical Toolbox. *J. Cheminf.* **2011**, DOI: doi:10.1186/1758-2946-3-33.
(73) Frisch, M. J. et al. *Gaussian 09, Revision A.1*; Gaussian, Inc.: Wallingford, CT, 2009.
(74) Dewar, M. J. S.; Zoebisch, E. G.; Healy, E. F.; Stewart, J. J. P. Development and Use of Quantum Mechanical Molecular Models. 76. AM1: A New General Purpose Quantum Mechanical Molecular Model. *J. Am. Chem. Soc.* **1985**, *107*, 3902−3909.
(75) Moitessier, N.; Englebienne, P.; Lee, D.; Lawandi, J.; Corbeil, C. R. Towards the Development of Universal, Fast and Highly Accurate Docking/scoring Methods: a Long Way to Go. *Br. J. Pharmacol.* **2008**, *153*, S7−S26.
(76) Hess, B.; Bekker, H.; Berendsen, H. J. C.; Fraaije, J. G. E. M. LINCS: a Linear Constraint Solver for Molecular Simulations. *J. Comput. Chem.* **1997**, *18*, 1463−1472.
(77) Jorgensen, W. L.; Maxwell, D. S.; Tirado-Rives, J. Development and Testing of the OPLS All−Atom Force Field on Conformational Energetics and Properties of Organic Liquids. *J. Am. Chem. Soc.* **1996**, *118*, 11225−11236.
(78) Berendsen, H. J. C.; Grigera, J. R.; Straatsma, T. P. The Missing Term in Effective Pair Potentials. *J. Phys. Chem.* **1987**, *91*, 6269−6271.
(79) Bussi, G.; Donadio, D.; Parrinello, M. Canonical Sampling Through Velocity Rescaling. *J. Chem. Phys.* **2007**, *126*, 014101.
(80) Parrinello, M.; Rahman, A. Polymorphic Transitions in Single Crystals: a New Molecular Dynamics Method. *J. Appl. Phys.* **1981**, *52*, 7182−7190.
(81) Darden, T.; York, D.; Pedersen, L. Particle Mesh Ewald: an N×log(N) Method for Ewald Sums in Large Systems. *J. Chem. Phys.* **1993**, *98*, 10089−10092.
(82) Wang, J.; Cieplak, P.; Kollman, P. A. How Well Does a Restrained Electrostatic Potential (RESP) Model Perform in Calculating Conformational Energies of Organic and Biological Molecules? *J. Comput. Chem.* **2000**, *21*, 1049−1074.
(83) Cornell, W. D.; Cieplak, P.; Bayly, C. I.; Gould, I. R.; Merz, K. M.; Ferguson, D. M.; Spellmeyer, D. C.; Fox, T.; Caldwell, J. W.; Kollman, P. A. A Second Generation Force Field for the Simulation of Proteins, Nucleic Acids, and Organic Molecules. *J. Am. Chem. Soc.* **1995**, *117*, 5179−5197.
(84) Li, J.; Xing, J.; Cramer, C. J.; Truhlar, D. G. Accurate Dipole Moments from Hartree−Fock Calculations by Means of Class IV Charges. *J. Chem. Phys.* **1999**, *111*, 885−892.
(85) *Ligand Topologies*. http://gaznevada.iq.usp.br/wp-content/uploads/opls_site.tar.gz (accessed May 2014).
(86) Jones-Hertzog, D. K.; Jorgensen, W. L. Binding Affinities for Sulfonamide Inhibitors with Human Thrombin Using Monte Carlo Simulations with a Linear Response Method. *J. Med. Chem.* **1997**, *40*, 1539−1549.
(87) Zar, J. H. *Biostatistical Analysis*, 4th ed.; Prentice Hall: NJ, 1999.
(88) Reynolds, J. A.; Gilbert, D. B.; Tanford, C. Empirical Correlation Between Hydrophobic Free Energy and Aqueous Cavity Surface Area. *Proc. Natl. Acad. Sci. U. S. A.* **1974**, *71*, 2925−2927.
(89) Chen, W.; Gilson, M. K.; Webb, S. P.; Potter, M. J. Modeling Protein−Ligand Binding by Mining Minima. *J. Chem. Theory Comput.* **2010**, *6*, 3540−3557.
(90) Vanommeslaeghe, K.; Hatcher, E.; Acharya, C.; Kundu, S.; Zhong, S.; Shim, J.; Darian, E.; Guvench, O.; Lopes, P.; Vorobyov, I.; Mackerell, A. D., Jr. CHARMM General Force Field: a Force Field for Drug−like Molecules Compatible with the CHARMM All−Atom Additive Biological Force Fields. *J. Comput. Chem.* **2010**, *31*, 671−690.
(91) Mulder, F. A. A.; Hon, B.; Muhandiram, D. R.; Dahlquist, F. W.; Kay, L. E. Flexibility and Ligand Exchange in a Buried Cavity Mutant of T4 Lysozyme Studied by Multinuclear NMR. *Biochemistry* **2000**, *39*, 12614−12622.
(92) Seeliger, D.; de Groot, B. L. Conformational Transitions upon Ligand Binding: Holo−Structure Prediction from Apo Conformations. *PLoS Comput. Biol.* **2010**, *6*, e1000634.
(93) Graves, A. P.; Brenk, R.; Shoichet, B. K. Decoys for Docking. *J. Med. Chem.* **2005**, *48*, 3714−3728.